2012-04-10

Dichotomous effects of VEGF-A on adipose tissue dysfunction

PROCEEDINGS OF THE NATIONAL ACADEMY OF SCIENCES OF THE UNITED STATES OF AMERICA, WASHINGTON, v. 109, n. 15, pp. 5874-5879, APR 10, 2012
http://www.producao.usp.br/handle/BDPI/33711

Dichotomous effects of VEGF-A on adipose tissue dysfunction

Kai Sun[a], Ingrid Wernstedt Asterholm[a,1], Christine M. Kusminski[a,1], Ana Carolina Bueno[a,b], Zhao V. Wang[a], Jeffrey W. Pollard[c], Rolf A. Brekken[d], and Philipp E. Scherer[a,e,2]

[a]Department of Internal Medicine, Touchstone Diabetes Center, [e]Department of Cell Biology, and [d]Hamon Center for Therapeutic Oncology and Division of Surgical Oncology, University of Texas Southwestern Medical Center, Dallas, TX 75390; [b]Department of Pediatrics, School of Medicine of Ribeirao Preto, University of Sao Paulo, Ribeirao Preto, Brazil; and [c]Department of Developmental and Molecular Biology, Center of Reproductive Biology and Women's Health, Albert Einstein Cancer Center, Albert Einstein College of Medicine, Bronx, NY 10461

Edited* by Roger H. Unger, Touchstone Center for Diabetes Research, Dallas, TX, and approved February 29, 2012 (received for review January 10, 2012)

Obese fat pads are frequently undervascularized and hypoxic, leading to increased fibrosis, inflammation, and ultimately insulin resistance. We hypothesized that VEGF-A–induced stimulation of angiogenesis enables sustained and sufficient oxygen and nutrient exchange during fat mass expansion, thereby improving adipose tissue function. Using a doxycycline (Dox)-inducible adipocyte-specific VEGF-A overexpression model, we demonstrate that the local up-regulation of VEGF-A in adipocytes improves vascularization and causes a "browning" of white adipose tissue (AT), with massive up-regulation of UCP1 and PGC1α. This is associated with an increase in energy expenditure and resistance to high fat diet-mediated metabolic insults. Similarly, inhibition of VEGF-A–induced activation of VEGFR2 during the early phase of high fat diet-induced weight gain, causes aggravated systemic insulin resistance. However, the same VEGF-A–VEGFR2 blockade in *ob/ob* mice leads to a reduced body-weight gain, an improvement in insulin sensitivity, a decrease in inflammatory factors, and increased incidence of adipocyte death. The consequences of modulation of angiogenic activity are therefore context dependent. Proangiogenic activity during adipose tissue expansion is beneficial, associated with potent protective effects on metabolism, whereas antiangiogenic action in the context of preexisting adipose tissue dysfunction leads to improvements in metabolism, an effect likely mediated by the ablation of dysfunctional proinflammatory adipocytes.

neovascularization | VEGF receptor 2 | hypoxia | obesity

Adipose tissue (AT) has unique plasticity, illustrated by its ability for rapid and dynamic expansion or reduction in periods of excess energy exposure or demand to ensure proper systemic energy homeostasis. AT expansion includes both hypertrophic and hyperplastic growth (1, 2). During the progression to chronic obesity, AT depots undergo profound pathological changes (3), such as enhanced oxidative damage, ER stress, local hypoxia, fibrosis, as well as immune cell infiltration and inflammation; many of these changes ultimately promote the development of insulin resistance (3).

However, not all AT expansion is associated with pathological changes. A subgroup of individuals that we refer to as "metabolically healthy obese" manage to expand their AT mass without the associated pathological consequences. The concept of "healthy AT expansion" suggests that fat pads differ largely with respect to how well they cope with the local tissue growth (3). In contrast to the pathological expansion widely seen upon weight gain, a healthy expansion consists of an enlargement of a given fat pad through recruitment of new adipocytes, along with the adequate development of the vasculature, minimal associated fibrosis, and the lack of hypoxia and inflammation (3).

AT is a highly vascularized tissue. Almost all adipocytes are surrounded by capillaries (4). A functional vascular system is critical for AT expansion. The macro- and microvasculature in AT supplies oxygen, nutrients, hormones, and growth factors, supporting expansion and homeostasis (4). The vasculature is also critical for the effective local removal of free fatty acids during fasting. Thus, angiogenesis has been considered to be a rate-limiting step for fat tissue expansion (3). Importantly, several crucial angiogenic factors, such as leptin, adiponectin, HGF-1, angiopoeitin-2, and VEGF-A are secreted by adipocytes, suggesting an autoregulatory function for angiogenesis in AT (4). Among them, VEGF-A is the only bona fide endothelial cell growth factor. VEGF-A accounts for most of the proangiogenic activity in AT (5, 6). VEGF-A binds to two tyrosine kinase receptors, VEGF receptors 1 (R1) and 2 (R2), prompting homo- and heterodimerization and becomes activated through transphosphorylation. VEGFR2 mediates most of the known cellular responses to VEGF. The function of VEGFR1 is less defined (7). VEGF-A levels in AT are regulated by exercise, hypoxia, insulin, a subset of cytokines, and several growth factors (8, 9). However, adipocytes frequently fail to mount a proper response to local hypoxia and do not produce sufficiently high levels of VEGF (10).

To date, a number of reports demonstrate that the disruption of neovascularization in AT prevents the development of obesity (11, 12). However, despite these efforts, much remains to be learned about targeting established blood vessels in the metabolically challenged AT (4, 11) and the role of angiogenesis and its regulation in healthy expanding fat tissue. This is especially true for the early stages of tissue expansion. Even though the literature has primarily focused on the inhibition of angiogenesis at later stages of metabolic dysfunction, we hypothesized that enhanced neovascularization in expanding fat pads should have beneficial effects. To test this hypothesis, we used a doxycycline (Dox)-inducible mouse model that allows us to overexpress VEGF-A uniquely in white adipose tissue at early stages of a high fat diet (HFD) challenge. We find that angiogenesis facilitates healthy fat pad expansion, reflected by smaller average size of adipocytes, absence of hypoxia, minimal fibrosis, and essentially none of the hallmarks of inflammation characteristic of dysfunctional AT. The mice remain metabolically fit on a HFD, with improved insulin sensitivity and increased energy expenditure. More importantly, VEGF-A also up-regulates UCP-1 and PGC1α levels, prompting white adipose tissue to assume a phenotype resembling more closely brown adipose tissue (13). In contrast, when we blocked functional blood vessel expansion by using the anti-VEGF antibody (Mcr84) that specifically inhibits binding of VEGF-A to VEGF receptor 2 at the initial stages of HFD feeding, we found that the mice showed a significant

Author contributions: K.S., I.W.A., C.M.K., and P.E.S. designed research; K.S., I.W.A., C.M.K., and A.C.B. performed research; Z.V.W., J.W.P., and R.A.B. contributed new reagents/analytic tools; Z.V.W. generated the mouse model; K.S., I.W.A., C.M.K., and P.E.S. analyzed data; and K.S., I.W.A., C.M.K., and P.E.S. wrote the paper.

The authors declare no conflict of interest.

*This Direct Submission article had a prearranged editor.

[1]I.W.A. and C.M.K. contributed equally to this work.

[2]To whom correspondence should be addressed. E-mail: philipp.scherer@utsouthwestern.edu.

This article contains supporting information online at www.pnas.org/lookup/suppl/doi:10.1073/pnas.1200447109/-/DCSupplemental.

metabolic impairment and reduced insulin sensitivity. However, using the neutralizing antibody in *ob*/*ob* mice with preexisting metabolic dysfunction resulted in the opposite effect: the blockade decreased local inflammation in epididymal white adipose tissue (EWAT), improved insulin sensitivity, and overall metabolic health. Taken together, these results highlight the complexity of interfering with angiogenesis in adipose tissue.

Results

Generation of Transgenic Mice with AT-Specific Expression of VEGF-A. Fig. S1*A* shows a schematic representation of the mouse model. The tetracycline responsive element (TRE)-driven VEGF-A transgenic model has been described previously (14). In our model, the TRE is regulated by the reverse tetracycline-dependent transcriptional activator (rtTA), whose expression is under the control of the AT specific adiponectin promoter (15). VEGF-A in the double transgenic mouse is induced in the presence of Dox. To induce VEGF-A within a physiological range, we titrated different doses of Dox as food admixtures from 600 mg/kg to 60 mg/kg. We avoided high doses of Dox (600 mg/kg) to circumvent pathological changes associated with supraphysiological local levels of VEGF.

By titrating the effective doses of Dox, we identified that lower levels of Dox (60 mg/kg) induced VEGF-A within a physiological range without causing edema formation. All subsequent experiments were performed at these lower doses. Expression of VEGF-A in a number of fat pads was assayed in the presence or absence of 60 mg/kg Dox treatment. In EWAT, the transgenic VEGF-A mRNA levels were induced in the Dox-treated double transgenic mice only, whereas VEGF-A levels were undetectable in mice carrying either one of the transgenes as well as double transgenic mice without Dox treatment (Fig. S1*B*). VEGF-A was predominantly induced in white adipose tissues (WATs) (Fig. S1*C*), whereas only moderate induction was seen in brown AT (BAT). No induction was observed in other tissues, such as the liver (Fig. S1*C*). Circulating VEGF-A levels were not significantly increased (Fig. S1*D*). Taken together, our system allows inducible expression of VEGF-A, with expression restricted to ATs.

Overexpression of VEGF-A Promotes Local Angiogenesis in WAT. Confocal fluorescent imaging reveals that compared with the control group, a higher vessel density is seen in the subcutaneous WAT (SWAT) of VEGF-A Tg mice (Fig. 1*A*). This differential vessel density is not observed in other tissues, e.g., in BAT (Fig. 1*A*), confirming the specificity of the VEGF-A effect in WAT. We then examined the levels of endothelial cell marker CD31. mRNA levels of CD31 were significantly induced in SWAT (Fig. 1*B*). The primers for q-PCR are listed in Table S1. Immunohistochemical analysis further confirmed enhanced CD31 staining in transgenic mice (Fig. 1*C*). Analysis of SWAT with anti-VEGF R2 antibodies also revealed an increased signal in the VEGF Tg mice (Fig. 1*D*). More importantly, our analysis with antiphospho-specific VEGFR2 also reveals more signal intensity in the SWATs of Tg mice (Fig. 1*D*). Activation of VEGF-A receptor 2 is considered to be a critical mediator of VEGF-A triggered proangiogenic function (16).

Overexpression of VEGF-A in AT Improves Glucose Tolerance and Insulin Sensitivity in HFD Challenged Mice. VEGF-A Tg mice weighed slightly less than control mice as we monitored body weights beyond week 7 (Fig. S2*A*). The modest body weight difference is due to a difference in fat mass in the VEGF-A Tg mice (Fig. S2*A*). Importantly, there were no signs of vascular leakage or edema formation, because NMR measurements show no difference in interstitial fluid in the transgenic mice (Fig. S2*A*). Both white fat pads examined (EWAT and SWAT) showed an increased density in vascular perfusion that is apparent, even at the level of the whole tissue, as judged by the darker color of both pads (Fig. S2*B*). The fasting levels of blood glucose and insulin were lower in transgenic mice (Fig. S2*D*). Five weeks after the initial HFD exposure, there were not yet any body weight differences between the groups. The oral glucose tolerance tests (OGTTs) demonstrate that in response to the glucose challenge, glucose tolerance in the VEGF-A Tg mice is significantly improved (Fig. 2*A*). Insulin sensitivity, as measured by insulin tolerance tests (ITTs), was also improved in the VEGF-A Tg mice (Fig. S2*C*). These results indicate a high degree of metabolic resistance to a HFD challenge upon supplementation of VEGF-A.

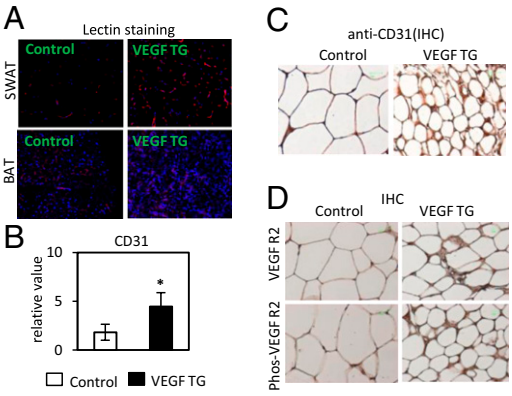

Fig. 1. VEGF-A stimulates angiogenesis in WAT. (*A*) Functional blood vessels in SWAT and BAT visualized by tail-injected rhodamine tagged lectin-1 in VEGF-A Tg and control mice. Blood vessels are shown in red and the nuclei are in blue, visualized by DAPI staining. The images were captured with confocal microscope. (*B*) q-PCR analysis of CD31 in SWAT of VEGF-A Tg and control mice ($n = 4$ in controls; $n = 5$ in VEGF-A Tg). The difference was analyzed by Student's *t* test. $^*P < 0.05$. (*C*) Immunohistochemical analysis with α-CD31 in SWAT of VEGF Tg or their littermate controls. (Scale bar, 50 μm.) (*D*) Immunohistochemical analysis with α-VEGF receptor 2 and α-phosphorylated VEGF receptor 2 in SWAT in both VEGF Tg and controls. (Scale bar, 50 μm.)

Overexpression of VEGF-A in AT Promotes an Increase in Lipid Clearance and a Decrease in HFD-Induced Hepatic Steatosis. A lipid tolerance test showed that VEGF-A Tg mice cleared an oral lipid challenge much more efficiently than the littermate controls (Fig. S3*A*). Furthermore, both the cholesterol and free fatty acid

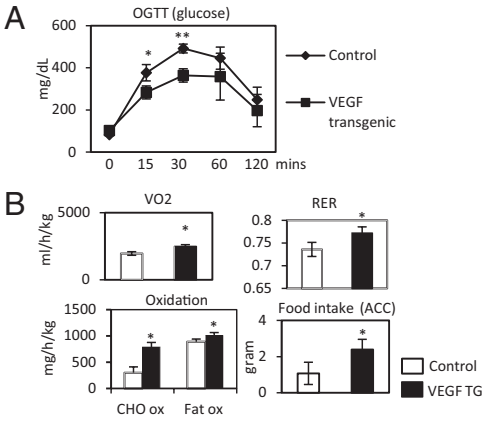

Fig. 2. VEGF-A Tg mice exhibit an improved metabolic profile. (*A*) Circulating glucose levels measured during an OGTT ($n = 5$ per group) 5 wk after HFD feeding. The difference at each time point was analyzed by Student's *t* test. $^*P < 0.05$; $^{**}P < 0.001$. (*B*) Indirect calorimetry was performed in a CLAMS system by housing mice after HFD plus Dox feeding for 6 wk. VO2 and RER (VCO_2/VO_2) were calculated from the average results during a 24-h light and dark cycle. Absolute contributions of carbohydrate and lipid metabolism to total energy expenditure and accumulated food intake were measured (ACC). $^*P < 0.05$; $^{**}P < 0.001$.

PHYSIOLOGY

(FFA) content in the livers were significantly lower in the VEGF-A Tg mice. Liver triglyceride (TG) levels also show a trend toward a decrease (Fig. S3*C*). H&E staining indicates fewer and smaller lipid droplets in hepatocytes from VEGF-A transgenic mice (Fig. S3*D*). Systemically, the improvements in lipid metabolism resulted in lowered plasma FFAs (Fig. S3*B*). The improvements in lipid parameters are, at least in part, due to higher levels of lipoprotein lipase (LPL), because mRNA levels of LPL in both adipose tissue and in the heart increased significantly (Fig. S3*E*). Collectively, these data highlight that AT VEGF overexpression results in significant systemic improvements in lipid metabolism.

Overexpression of VEGF-A in AT Leads to an Increase in Energy Expenditure. The energy expenditure in metabolic chambers data indicate that the rate of oxygen consumption (VO_2) was significantly increased in the VEGF Tg mice (Fig. 2*B*). They also had a significantly higher respiratory exchange rate (RER), indicating that a higher proportion of energy expended in the transgenics derives from glucose metabolism (Fig. 2*B*). However, the absolute rate of lipid oxidation is similar between VEGF Tg and their littermate controls, whereas the use of carbohydrate is increased in the VEGF Tg mice (Fig. 2*B*). VEGF-A overexpression leads therefore to an increase in energy expenditure, and the increase is primarily driven by an increase in carbohydrate metabolism. Moreover, VEGF Tg mice have an increase in food intake (Fig. 2*B*), further illustrating the higher energy turnover in light of the weight differences.

Overexpression of VEGF-A Decreases Adipocyte Size and Enhances a "Brown Adipose" Phenotype in WAT. Histological examination revealed dramatic differences, including smaller-sized adipocytes in WATs of VEGF Tg mice (Fig. 3*A* and Fig. S4*A*). Furthermore, the reduction of lipid depots and a more multilocular appearance of the SWAT cells are characteristic features of BAT (Fig. 3*A*; and see Fig. S6*B*). Indeed, both qPCR and Western blotting revealed marked increases in PGC-1α and UCP-1 levels (Fig. 3 *B* and *C* and Fig. S4*C*), lending further support for a browning of WATs in the VEGF-A Tg mice (13, 17). We also observed that mRNA levels for PPARγ and ZFP423 were unaffected (Fig. S4*B*). In VEGF Tg mice, leptin levels in both AT and serum were significantly decreased (Fig. S5*A*). Even though there was no difference at the level of adiponectin mRNA (Fig. S5*B*), circulating adiponectin levels decreased slightly, whereas intracellular pools were increased (Fig. S5 *C* and *D*), suggestive of a reduction in adiponectin secretion.

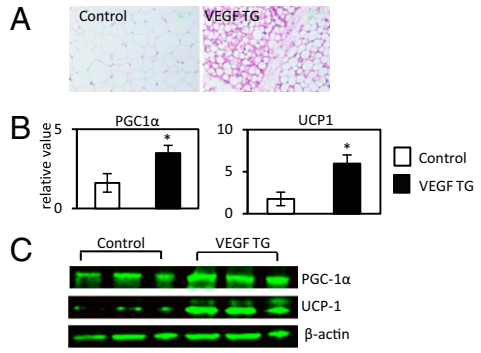

Fig. 3. VEGF-A Tg mice have smaller white adipocytes with BAT-like properties. (*A*) H&E staining of SWAT of VEGF-A Tg mice after HFD plus Dox feeding for 8 wk. (Scale bars, 50 μm.) (*B*) q-PCR analysis of PGC-1α and UCP-1 in EWAT of VEGF-A Tg and their littermate controls. The readings are normalized to hypoxanthine phosphoribosyltransferase (HPRT). $*P < 0.05$; $**P < 0.001$. (*C*) Western blot analysis for both PGC-1α and UCP-1 in WAT of VEGF Tg and their littermate controls. Results were normalized with β-actin.

Overexpression of VEGF-A Suppresses Hypoxia and Fibrosis and Reduces Local Inflammation in WAT During HFD Exposure. Immunohistochemical assessment of local hypoxia using a hypoxyprobe indicates that hypoxia in WATs is significantly reduced in transgenic mice (Fig. 4*A*). Consistent with the reduction of hypoxic conditions, there is a significant reduction in the levels of HIF1α associated with induced VEGF-A overexpression (Fig. 4*B*). The fibrotic collagens III and VI (Col3 and Col6) are reduced (Fig. 4*B*). Interestingly, matrix metalloprotease-1 (MMP-1), one of the key enzymes facilitating the digestion of collagens in AT, was significantly induced in VEGF Tg mice (Fig. 4*B*). In line with these observations, a trichrome stain of SWAT and EWAT indicates that the extracellular matrix (ECM) accumulation is significantly reduced in the transgenic animals (Fig. S6*B*).

We further observed significantly decreased expression of inflammatory factors, such as IL6, F4/80, TNFα, and SAA3 by qPCR in EWAT of VEGF-A Tg mice (Fig. 4*C*). In line with these transcriptional changes, the levels of the generic plasma inflammatory marker serum amyloid A (SAA) were significantly reduced in VEGF Tg mice (Fig. S6*A*). Immunohistochemical analysis of both SWAT and EWAT with an anti-F4/80 antibody further confirms a reduced frequency of "crown-like" structures surrounding adipocytes in the VEGF-A Tg mice (Fig. 4*D* and Fig. S6*C*). Collectively, we conclude that local overexpression of VEGF-A in AT prevents tissue dysfunction.

Angiogenesis-Inhibitor Treatment During Early Stages of HFD-Induced Weight Gain Aggravates Systemic Metabolic Health. To investigate the "loss-of-function" effect of angiogenesis, we used anti-VEGF monoclonal antibody Mcr84. This monoclonal antibody binds mouse VEGF and selectively blocks VEGF from interacting with VEGFR2 (18). We treated 6-wk-old wild-type mice with Mcr84 or control IgG just before and throughout a 6-wk time course of HFD feeding. Whereas food intake, weight gain (Fig. S7*A*), and dissected fat pad size did not differ between groups, we observed an impaired response to the HFD in the Mcr84-treated mice. The Mcr84-treated mice required higher insulin to control their glucose levels during an OGTT (Fig. 5*B*), even though a comparable rate of glucose clearance was maintained, along with a reduction in lipid clearance (Fig. 5*C*). As a reflection of the dysfunctional ATs,

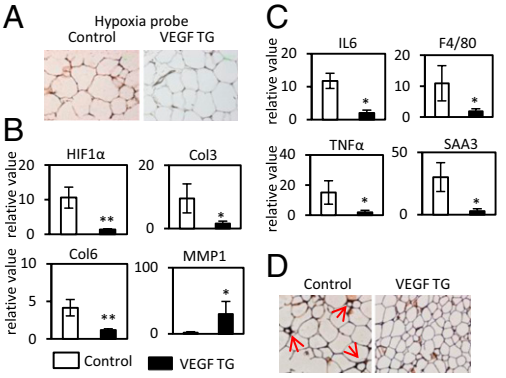

Fig. 4. VEGF-A overexpression ameliorates hypoxia, fibrosis, and inflammatory responses in WAT induced by HFD. (*A*) Immunohistochemical staining by hypoprobe-1 in WAT of VEGF Tg mice and their littermate controls after HFD plus Dox treatment for 8 wk. The darker staining on the *Left* indicates more hypoxic environment in controls. (*B*) q-PCR analysis of HIF-1α and its target collagen genes in EWAT. The readings are normalized to HPRT. $*P < 0.05$; $**P < 0.001$. (*C*) q-PCR analysis of inflammatory cytokines IL6, TNFα, SAA3, and macrophage marker F4/80 in EWAT. The readings are normalized to HPRT. $*P < 0.05$; $**P < 0.001$. (*D*) Immunohistochemical staining of F4/80 in SWAT of VEGF-A Tg mice. Red arrows indicate the crowns formed by accumulation of macrophages surrounding the dysfunctional adipocytes.

the circulating adiponectin levels were lower in Mcr84-treated mice (Fig. S7*C*). In an attempt to assess metabolic flexibility, we measured FFAs in the fed and fasted state. Control mice display the anticipated increase and decrease of FFAs during the fasted and fed state, respectively. However, this dynamic regulation was absent in the Mcr84-treated mice (Fig. 5*D*). As expected, Mcr84-treated WAT displays a reduction in the amount of fluorescently labeled lectin (Fig. 5*A*). We also observed that the mRNA levels of CD31 decreased in SWAT but not in livers (Fig. S7*B*), indicating that angiogenesis inhibition is primarily affecting fat tissues. Furthermore, there was an increase in macrophage infiltration in EWAT in the Mcr84-treated mice (Fig. S7*D*). Despite similar overall fat pad weight, we observed an increase in average adipocyte cell size in the Mcr84-treated mice (Fig. S7*D*).

Angiogenesis-Inhibitor Treatment in Dysfunctional AT Minimizes Body-Weight Gain and Enhances Insulin Sensitivity in the Context of *ob/ob* Mice. Our previous observations demonstrated the metabolically challenged state of WAT in adult *ob/ob* mice (10). We therefore selected 6-wk-old *ob/ob* mice as our model. During a 3-wk treatment regimen, Mcr84-treated *ob/ob* mice gained slightly less body weight than their control IgG-treated littermates (Fig. S8*A*). Furthermore, the Mcr84-treated *ob/ob* group displayed a trend toward improvement of glucose-tolerance compared with the control group (Fig. S9*B*). Upon examination of acute fasting serum parameters, circulating FFA levels were significantly lower in the Mcr84-treated *ob/ob* mice compared with control IgG-treated mice (Fig. S9*C*). Circulating glucose levels following an overnight fast were lower in Mcr84-treated *ob/ob* mice compared with controls (Fig. S9*C*). Furthermore, the mRNA expression levels of the macrophage marker F4/80 significantly decreased in the Mcr84-treated mice (Fig. S9*D*).

Consistent with these observations, immunofluorescence staining of EWAT shows that the anti–Mcr84-treated animals displayed a marked reduction in vascular density (Fig. S9*A*). Similarly, the mRNA levels of CD31were significantly downregulated in EWAT of anti–Mcr84-treated *ob/ob* mice (Fig. S8*B*). We also found a dramatic increase in adipocyte death as judged by the number of perilipin-negative lipid droplets in the AT of Mcr84-treated mice compared with control (Fig. S9*E*).

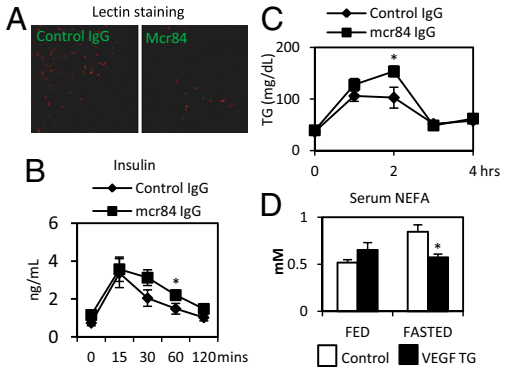

Fig. 5. Blockade of VEGF-A binding to VEGFR2 by Mcr84 accelerates metabolic dysfunction induced by HFD. (*A*) Functional blood vessels in AT labeled by rhodamine-tagged lectin. The mice were fed with HFD for 6 wk before the experiment. Mcr84 or control IgG were injected i.p at the initial stage and continued twice per week for the whole HFD feeding process. Blood vessels are shown in red and the nucleus in blue, by DAPI staining. (*B*) Insulin levels for an OGTT in Mcr84- or control IgG-treated mice (n = 5 per group) after antibody treated for 6 wk. *$P < 0.05$. (*C*) Triglyceride levels for a lipid clearance test in Mcr84- or control IgG-treated mice (n = 5 per group). *$P < 0.05$. (*D*) Serum nonesterified fatty acid (NEFA) levels in Mcr84- or control IgG-treated mice (n = 5 per group) after antibody treated for 7 wk. *$P < 0.05$.

Discussion

Angiogenesis is an integral component of adipose tissue physiology (12), even under conditions when weight is stable. In the past two decades, numerous proangiogenic factors, such as VEGF-A, leptin, adiponectin, angiopoietin-2, monobutyrin, FGF-2, and hepatocyte growth factor (HGF) have been identified in both WAT and BAT (3). Importantly, these factors were also found to be regulated by different physiological and pathological conditions. For example, VEGF-A levels in both local fat pads and circulation are up-regulated by hypoxia, high insulin levels, and exercise (3, 9). However, the complex crosstalk between angiogenesis and adipogenesis and the resulting metabolic effects are not well understood. In this study, we used an AT-specific, inducible VEGF-A expression system to delineate the process in detail. We induced VEGF-A expression upon initiating a HFD exposure, using a relatively low Dox concentration (60 mg/kg) to achieve a physiologically relevant degree of VEGF-A overexpression from adipose tissue. As a major endothelial cell regulator (16), VEGF-A enhances VEGFR2 phosphorylation and triggers angiogenesis, as reflected by an enhancement in vascular density in the WAT. Phenotypically, this results in global improvements in all aspects examined as they relate to glucose and lipid metabolism. The underlying mechanism for these improvements is likely to be related to the reduced hypoxia that is prevailing in the transgenic mice, paralleled by a lack in fibrosis and minimum local inflammation in the WAT of VEGF-A transgenic mice.

The transgenic mice consumed more oxygen and generated more carbon dioxide, suggesting they exhibit higher energy expenditure. Transgenic animals also had significantly higher RER values. Histological examination of the transgenic mice demonstrated a BAT-like phenotype in the WAT depots, particularly in SWAT. Along with the visually apparent changes, both qPCR and immunoblotting analysis of WAT revealed significant increases in PGC-1α and UCP-1 levels, which may be the key drivers for the BAT-like appearance of the WAT. Of high interest in this context is UCP-1, a protein that uncouples electron transport from ATP production to produce heat (19), thereby offering an explanation for the increased energy expenditure. An overall increase in the mitochondrial mass is stimulated by PGC-1α. Consistent with these findings is the observation by Xue et al. who reported that cold exposure in mice leads to a brown-like phenotype in WAT; they further found that AT up-regulates VEGF levels under these conditions and switches the fat pads to a more proangiogenic profile upon cold exposure (17). In this context, our observations underline the key role that VEGF-A plays in this process, because we observe a similar transition to a "BAT-like" phenotype in the presence of VEGF-A alone without an associated cold exposure.

Dysfunctional AT per se can lead to systemic insulin resistance (3). The subsequent increased release of free fatty acids and proinflammatory factors trigger an elevated degree of lipotoxicity in nonadipose tissue organs, particularly in liver and muscle (20). Indeed, we observed an increase of serum FFA and TG levels in both serum and liver in the control mice after HFD feeding. However, the transgenic mice showed lower lipotoxic side effects and normal liver histology. Because the VEGF transgene expression remained local within adipose tissue, it did not affect angiogenesis in the liver. Therefore, the improvements in lipid metabolism in the liver are a direct consequence of the beneficial effects of VEGF elevation in adipocytes. The underlying mechanisms leading to the unexpected decrease in circulating adiponectin levels, potentially as a function of impaired release from adipocytes in the VEGF-A TG model, are currently under investigation.

In contrast, blocking angiogenesis at early stages of obesity during the increase in AT mass is rather different. We treated wild-type mice with the VEGF-A Mcr84 antibody or control IgGs just before and throughout a 6-wk time course of high fat diet feeding. Mcr84-treated WAT displays a reduction in vascular density, whereas liver and other tissues were unaffected.

This indicates that our antiangiogenesis treatment is effective enough to have an impact on vascular density, but only in AT despite systemic exposure to antibody. This further highlights that adipose tissue is one of the tissues that constantly remodels its vasculature. It is thereby particularly susceptible to an imbalance of proangiogenic signals. Despite similar overall fat pad weights, we observed an increase in adipocyte cell size in the antibody-treated mice. Furthermore, there was an increase in macrophage infiltration in EWAT. Whereas food intake, weight gain, and dissected fat pad size did not differ between groups, we observed that Mcr84-treated mice required higher insulin to control their glucose levels during an OGTT, and their lipid clearance ability was also decreased. As an additional indicator of the dysfunctionality of fat cells, the circulating adiponectin levels displayed a trend toward a decrease. Importantly, whereas control mice displayed the anticipated increase and decrease of FFA during feeding/fasting, this dynamic regulation was absent in the Mcr84-treated mice. This clearly highlights the relevance of proper vascular expansion during weight gain.

Several reports have suggested that antiangiogenic treatment regimens reduce body weight in murine models of obesity and lead to improvements in some aspects of the metabolic syndrome (21–23). Thus, both enhancing AT angiogenesis in our present study and inhibiting AT angiogenesis are paradoxically associated with an improvement in systemic metabolism. Although the underlying mechanism for angiogenesis inhibitor-induced improvements on metabolic parameters is still not clear, we hypothesized that blocking the capacity for angiogenesis may have different outcomes, dependent on the stage of obesity. Previous studies with angiogenesis inhibitors were performed in extremely obese mice, not in the early stages of diet-induced weight gain. Moreover, dysfunctional adipocytes display an inefficient TG storage. The elevated lipolytic rate under these conditions is less capable of sequestering and neutralizing excess FFAs. This leads to ectopic lipid storage, increased inflammation, and further deterioration of systemic insulin sensitivity (20). Blocking the capacity for angiogenesis in the context of severe obesity induces adipocyte apoptosis (21). We suggest that the largest and most dysfunctional adipocytes are most likely to undergo angiogenesis-inhibitor–induced apoptosis compared with smaller adipocytes, because they already are under hypoxic conditions. By blocking the capacity for angiogenesis, angiogenesis inhibitors may reduce the proinflammatory contributions of an excessive number of dysfunctional adipocytes on systemic metabolism. Indeed, our experiments in *ob*/*ob* mice support this hypothesis: treating *ob*/*ob* mice with Mcr84 that selectively blocks VEGF-A from activating VEGFR2 causes increased adipocyte death. In parallel, the systemic serum inflammatory factor SAA decreases significantly. Systemically, the mice exhibit weight loss with a concomitant improvement in glucose tolerance. We selected 6-wk-old *ob*/*ob* mice as an "unhealthy expansion model," such that we and others have demonstrated that WAT in these mice undergoes hypoxia along with induced HIF1α expression, which in turn stimulates fibrosis and local inflammation (10, 24). Indeed, other studies have similarly suggested that VEGF inhibitor treatment, which specifically targets VEGFR2, decreases AT mass following HFD (7).

In conclusion, our findings highlight how manipulation of angiogenesis at various stages of obesity development differentially affects whole AT physiology and energy expenditure. Specifically, stimulation of angiogenesis at an early stage of obesity has beneficial effects in mice, whereas angiogenesis inhibition after the fact also supports improvements, but with a different underlying mechanism. Our studies pave the way for a better understanding of these phenomena that give rise to profound effects of angiogenesis on overall healthy condition and energy expenditure. Given that this aspect of adipose tissue physiology translates well to the clinical setting, it is tempting to speculate whether it is worthwhile to supplement patients with VEGF-A in the obese state. However, as with many other pharmacological interventions aimed at improving adipose tissue health, we have to be concerned that the same strategies will enhance the growth of solid tumors, as they rely on similar rate-limiting steps for expansion as a growing adipose tissue pad.

Materials and Methods

Animals. TRE–VEGF-A transgenic mice have been described previously (14). Mice in the original Friend leukemia virus B strain (FVB) background have been backcrossed to pure C57BL/6 mice (Jackson Laboratories) for eight generations to obtain a pure C57BL/6 background. *ob*/*ob* experiments were performed on mice on a pure FVB background. Adiponectin-rtTA transgenic mice were on a pure C57BL/6 background. These mice were crossed with TRE–VEGF-A mice to generate the AT-specific Dox-inducible VEGF-A transgenic mice. All experiments were conducted using littermate-controlled male mice and were started when they were 5 wk old. Mice were housed in cages with 12-h dark–light cycle with free access to water and regular chow. All animal experiments were performed with the approval of the institutional animal care and use committee of University of Texas Southwestern Medical Center at Dallas.

Mcr84 (Anti-VEGF) Treatment. The VEGF-specific antibody Mcr84 had been described previously (18). For the treatment of wild-type mice, 6-wk-old male C57B/6 wild-type mice were injected intraperitoneally (i.p.) with Mcr84 or isotype control IgGs (0.2 mg per mouse) twice per week. The injection began just before the introduction of HFD and continued for 6 wk. Food intake and body weights were monitored throughout the entire time course. An oral glucose and lipid tolerance test were performed after 4 and 5 wk on HFD, respectively. At week 6, the mice were fasted for 3 h and anesthetized with isoflurane. Tissues and sera were collected for analysis. Similarly, for the experiments in *ob*/*ob* mice, 6-wk-old male *ob*/*ob* mice were injected i.p. with either control IgG or mcr84 twice per week for 3 wk.

Statistical Analysis. All results are given as means ± SEM. Differences between two groups were examined for statistical significance with Student's *t* test. Significance was accepted at a P value of <0.05.

Additional Materials and Methods. Please refer to *SI Materials and Methods*.

ACKNOWLEDGMENTS. We thank members in the P.E.S. laboratory, especially Dr. Nils Halberg, for discussion and technical help; the pathology core facility at University of Texas (UT) Southwestern for help with histology; Dr. Bob Hammer and the transgenic core facility at UT Southwestern for generating the adiponectin-rtTA transgenic mice; the Metabolic Core Unit at UT Southwestern for phenotyping efforts; and Steven Spurgin for help with manuscript preparation. This work was supported by National Institutes of Health Grants R01-DK55758, RC1DK086629, and P01DK088761 (to P.E.S.).

1. Rosen ED, MacDougald OA (2006) Adipocyte differentiation from the inside out. *Nat Rev Mol Cell Biol* 7:885–896.
2. Sethi JK, Vidal-Puig AJ (2007) Thematic review series: Adipocyte biology. Adipose tissue function and plasticity orchestrate nutritional adaptation. *J Lipid Res* 48:1253–1262.
3. Sun K, Kusminski CM, Scherer PE (2011) Adipose tissue remodeling and obesity. *J Clin Invest* 121:2094–2101.
4. Cao Y (2010) Adipose tissue angiogenesis as a therapeutic target for obesity and metabolic diseases. *Nat Rev Drug Discov* 9:107–115.
5. Zhang QX, et al. (1997) Vascular endothelial growth factor is the major angiogenic factor in omentum: Mechanism of the omentum-mediated angiogenesis. *J Surg Res* 67:147–154.
6. Hausman GJ, Richardson RL (2004) Adipose tissue angiogenesis. *J Anim Sci* 82:925–934.
7. Tam J, et al. (2009) Blockade of VEGFR2 and not VEGFR1 can limit diet-induced fat tissue expansion: Role of local versus bone marrow-derived endothelial cells. *PLoS ONE* 4:e4974.
8. Liekens S, De Clercq E, Neyts J (2001) Angiogenesis: Regulators and clinical applications. *Biochem Pharmacol* 61:253–270.
9. Zwetsloot KA, Westerkamp LM, Holmes BF, Gavin TP (2008) AMPK regulates basal skeletal muscle capillarization and VEGF expression, but is not necessary for the angiogenic response to exercise. *J Physiol* 586:6021–6035.
10. Halberg N, et al. (2009) Hypoxia-inducible factor 1alpha induces fibrosis and insulin resistance in white adipose tissue. *Mol Cell Biol* 29:4467–4483.
11. Daquinag AC, Zhang Y, Kolonin MG (2011) Vascular targeting of adipose tissue as an anti-obesity approach. *Trends Pharmacol Sci* 32:300–307.
12. Rupnick MA, et al. (2002) Adipose tissue mass can be regulated through the vasculature. *Proc Natl Acad Sci USA* 99:10730–10735.
13. Kajimura S, et al. (2008) Regulation of the brown and white fat gene programs through a PRDM16/CtBP transcriptional complex. *Genes Dev* 22:1397–1409.

14. Lin EY, et al. (2007) Vascular endothelial growth factor restores delayed tumor progression in tumors depleted of macrophages. *Mol Oncol* 1:288–302.
15. Wang ZV, Deng Y, Wang QA, Sun K, Scherer PE (2010) Identification and characterization of a promoter cassette conferring adipocyte-specific gene expression. *Endocrinology* 151:2933–2939.
16. Sato Y, et al. (2000) Properties of two VEGF receptors, Flt-1 and KDR, in signal transduction. *Ann N Y Acad Sci* 902:201–205, discussion 205–207.
17. Xue Y, et al. (2009) Hypoxia-independent angiogenesis in adipose tissues during cold acclimation. *Cell Metab* 9:99–109.
18. Sullivan LA, et al. (2010) r84, a novel therapeutic antibody against mouse and human VEGF with potent anti-tumor activity and limited toxicity induction. *PLoS ONE* 5: e12031.
19. Cannon B, Nedergaard J (2004) Brown adipose tissue: Function and physiological significance. *Physiol Rev* 84:277–359.
20. Unger RH, Clark GO, Scherer PE, Orci L (2010) Lipid homeostasis, lipotoxicity and the metabolic syndrome. *Biochim Biophys Acta* 1801:209–214.
21. Kolonin MG, Saha PK, Chan L, Pasqualini R, Arap W (2004) Reversal of obesity by targeted ablation of adipose tissue. *Nat Med* 10:625–632.
22. Dallabrida SM, Rupnick MA (2002) Vascular endothelium in tissue remodeling: Implications for heart failure. *Cold Spring Harb Symp Quant Biol* 67:417–427.
23. Bråkenhielm E, et al. (2004) Angiogenesis inhibitor, TNP-470, prevents diet-induced and genetic obesity in mice. *Circ Res* 94:1579–1588.
24. Hosogai N, et al. (2007) Adipose tissue hypoxia in obesity and its impact on adipocytokine dysregulation. *Diabetes* 56:901–911.